Photolysis of Polycyclic Aromatic Hydrocarbons on Water and Ice Surfaces

T. F. Kahan and D. J. Donaldson*

Department of Chemistry, University of Toronto, 80 Saint George Street, Toronto, Ontario, Canada M5S 3H6

Received: October 10, 2006; In Final Form: December 22, 2006

Laser-induced fluorescence detection was used to measure photolysis rates of anthracene and naphthalene at the air−ice interface, and the kinetics were compared to those observed in water solution and at the air−water interface. Direct photolysis proceeds much more quickly at the air−ice interface than at the air−water interface, whereas indirect photolysis due to the presence of nitrate or hydrogen peroxide appears to be suppressed at the ice surface with respect to the liquid water surface. Both naphthalene and anthracene self-associate readily on the ice surface, but not on the water surface. The increase in photolysis rates observed on ice surfaces is not due to this self-association, however. The wavelength dependence of the photolysis indicates that it is due to absorption by the PAH. No dependence of the rate on temperature is seen, either at the liquid water surface or at the ice surface. Molecular oxygen appears to play a complex role in the photolytic loss mechanism, increasing or decreasing the photolysis rate depending on its concentration.

Introduction

Ice and snow are important physical and chemical sinks for a wide variety of pollutants, in both urban and remote areas. Many contaminants are deposited in high-latitude snowpacks via long-range transport, while other compounds are formed by chemical reactions in snow or ice. The photochemistry of PAHs in ice has been studied in the context of astrochemistry, using Lyman-α and other high-energy radiation sources (see for instance refs 1 and 2), but interest in photochemical transformations of pollutants in or on frozen media under atmospherically relevant conditions on Earth is much more recent. The photochemistry of compounds that affect polar boundary layer ozone concentrations,[3−8] such as halides and nitrate, have received a good deal of attention recently. Much less is known about the near-UV photochemical transformations of organic pollutants in frozen media, although small hydrocarbons including alkanes, alkenes, ketones, and carboxylic acids in high latitude regions are suspected of being formed at least partially through photolysis in snow,[9−11] and laboratory studies have shown that larger organic compounds undergo photolysis in ice.[12−14]

Frozen water presents a complex and poorly understood reaction medium,[15] due in part to the existence of a quasi-liquid layer (QLL) at its surface. The QLL is a region close to the air−ice interface where the water molecules' positions become more random and the structure of the ice matrix becomes disordered, in a manner somewhat resembling that of liquid water. Pollutants deposited on ice surfaces from the gas phase are likely to be found primarily in the QLL, and it has been suggested that exclusion during freezing could also result in extremely high concentrations of pollutants in the QLL.[5,13,14,16−18]

The environment presented by the QLL to chemical reagents is not well understood. Measurements of physical properties of the QLL such as its density, the orientation of its water molecules, and the temperature dependence of its depth give widely different results depending on the measurement technique.[19−26] It is generally agreed that the thickness of the QLL increases with increasing temperature, and that the orientation and density of the water molecules are different than they are at the liquid water surface even at temperatures very close to the melting point. A recent review[27] contains a more detailed discussion. In addition to a poor understanding of the physical properties of the QLL, the manner in which pollutants interact with it while undergoing chemical transformation is not known. Rate enhancements in frozen aqueous and organic solvents have been observed for many bimolecular reactions; these have been attributed to high concentrations of reagents, as a result of their exclusion during freezing.[28] Whether a rate enhancement may also exist for photochemical reactions is not clear. While the photolysis of small inorganic compounds such as nitrate and hydrogen peroxide appears to proceed in a similar fashion in ice as in water,[5,18] very little information regarding the photolysis of organic molecules associated with ice is available.[12−15,29] Comparative kinetics of organic pollutants in liquid and solid aqueous media have not widely been measured,[12,30] and there continues to be debate as to whether the photolysis of organic compounds occurs in the QLL, in the ice matrix, or in both.[12−14]

In the present study we compare photolysis rates of PAHs at liquid and solid air−aqueous interfaces. This allows us to address two major questions: (i) does photochemistry occur at the ice surface (i.e., in the QLL) and (ii) how similar is the photochemistry of large organic molecules at the air−ice interface to that observed in liquid water?

Experimental Section

Apparatus. Figure 1 shows the reaction chamber used for this study. It consists of a ∼500 mL Teflon box with side ports through which gases can be introduced and vented. The bottom of the chamber consists of a copper plate that is soldered to copper tubing, through which cooling fluid is circulated. The temperature of the plate is monitored by using a thermistor attached to its surface; good thermal contact is assured by using thermal grease. Experiments were carried out at temperatures ranging from −16 to 24 °C. Some experiments conducted at room temperature did not use the circulating cooling liquid; an

* Address correspondence to this author. E-mail: jdonalds@chem.utoronto.ca.

10.1021/jp066660t CCC: $37.00
Published on Web 01/26/2007

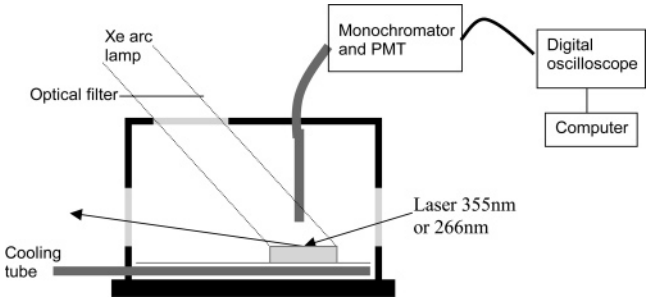

Figure 1. Schematic representation of the reaction chamber and experimental setup.

increase of ~2 °C over the course of a photolysis experiment (ca. 2 h) was observed. For all other experiments, the temperature remained constant to within 0.4 °C during the kinetics measurements.

Anthracene was excited at 355 nm and naphthalene at 266 nm by the frequency-tripled or -quadrupled output of a pulsed Nd:YAG laser operating at a repetition rate of 10 Hz. Pulse energies were less than 0.5 mJ for all experiments. The unfocussed laser beam entered and exited the chamber through quartz windows situated at either end of the chamber and impinged the surface of the sample at a glancing angle (ca. 75° from the surface normal). Fluorescence of surface species excited by the laser was collected perpendicular to the surface with use of a 7 mm diameter liquid light guide suspended 1 cm above the sample. The fluorescence was imaged into a monochromator, and the transmitted intensity was detected by a photomultiplier tube and sent to a digital oscilloscope and computer for analysis. The digital oscilloscope averaged the intensity vs time signal over 64 laser shots and these data were sampled and stored by the computer.

The photolysis light source was a 75 W xenon arc lamp whose output was directed through a quartz window in the top plate of the chamber onto the sample. With the exception of experiments designed to measure the wavelength dependence of the kinetics, this light passed through a 295 nm long-pass optical filter prior to entering the chamber. With this filter in place, the total radiant power entering the chamber was ~0.2 W, as measured by a power meter with an energy-absorbing head.

Sample Preparation. Liquid samples were prepared in one of three ways: They were placed in a petrie dish, held in a 10 mm path length quartz cuvette, or in a circular quartz cell with a depth of 7 mm and a 1 cm radius. Ice samples were prepared by freezing ~0.5 mL of water either on a small copper plate or in the quartz cell; the surface area of the ice exposed to the air was ~3 cm^2 in both cases. We assume always that the thermistor provides an accurate indication of the sample temperature.

Two methods were used to prepare PAH samples for study. In the first, a few grams of the solid PAH were placed in a container that was immersed in a constant temperature bath maintained at ~75 °C. Prepurified dry N_2 flowed through the container at a rate of (1.2 ± 0.3) L min^{-1}, as determined by a mass flow meter. The resulting mixture of PAH and N_2 flowed through ~50 cm of room temperature $^1/_4$ in. Tygon tubing before entering the sample chamber through an opening in the roof of the chamber. In the second method, samples of known concentration were prepared by diluting a saturated aqueous solution of PAH to concentrations on the order of 10^{-8}−10^{-7} M. For experiments on ice, this solution was either frozen or a few drops (~25 μL total) were deposited from a pasteur pipet onto the surface of an existing ice sample. Anthracene was also deposited on ground glass microscope slides by depositing 15−110 μL of an anthracene-in-methanol solution of known concentration on the slide and allowing the methanol to evaporate.

Liquid samples containing nitric acid and hydrogen peroxide were prepared by adding the reagent volumetrically to an aqueous anthracene solution. Hydrogen peroxide was introduced to the ice samples by spreading a small quantity of a hydrogen peroxide solution of known concentration over the ice surface prior to depositing the anthracene solution on the ice. Nitric acid was introduced to ice samples either in the manner described above for hydrogen peroxide or by depositing gaseous nitric acid onto the ice sample already containing anthracene. This was done by withdrawing a volume ranging from 0.2 to several mL of vapor from the headspace of a bottle containing concentrated nitric acid with a pasteur pipet or a microliter syringe, and then expelling the collected gas onto the ice surface. On the basis of the vapor pressure expression for 70 wt % nitric acid solutions given by Hanson and Mauersberger[31] and confirmed by ion chromatograph measurements performed in this lab,[32] 0.25 mL of vapor above a room temperature 70 wt % nitric acid solution is expected to contain approximately 1×10^{16} molecules. If all this nitric acid adsorbed to the ice surface, this would result in a coverage of ~3×10^{15} molecules cm^{-2}.

Most ice samples were prepared in an atmosphere of air. Photolysis was also carried out under an ambient atmosphere, except when the PAH was introduced from the gas phase in a stream of nitrogen. To determine the effects of oxygen on the photolysis kinetics, reactions were also carried out under atmospheres of pure oxygen and pure nitrogen. For these studies, the reaction chamber was purged with the appropriate gas for 30 min prior to introducing the anthracene from the gas phase. For the reactions on ice, N_2 or O_2 was flowed through the chamber during sample freezing as well as during PAH deposition and irradiation.

Fluorescence Spectra. Wavelength-resolved fluorescence spectra of anthracene and naphthalene were acquired at the sample surface. The monochromator was manually scanned to monitor laser-induced fluorescence intensity at approximately 3 nm intervals over the wavelength ranges of interest. Fluorescence spectra of anthracene and naphthalene in bulk aqueous or methanol solutions were acquired on a commercial spectrofluorimeter at excitation wavelengths of 355 and 266 nm, respectively.

Kinetics Studies. Kinetics at the air−ice and air−water interfaces were obtained in situ with the laser induced fluorescence technique described above. Fluorescence intensity was recorded at various intervals over a period ranging from 30 to 150 min, depending on the sample. Prior to irradiating the sample, the fluorescence intensity was monitored over the span of several minutes to ensure the stability of the signal. The sample was then exposed to radiation from the Xenon arc lamp. Data were collected until the fluorescence intensity no longer decreased with time. Anthracene fluorescence was monitored at 379, 403, or 420 nm, and naphthalene fluorescence was monitored at 333 nm.

Naphthalene photolysis kinetics in water were obtained by irradiating aqueous naphthalene solutions in a 10 mm path length quartz cuvette; fluorescence spectra were acquired at 20 min intervals using a commercial spectrometer.

Chemicals. All chemicals were used as delivered. Anthracene and 1-decanol were purchased from Sigma-Aldrich and had stated purities of 99%. Naphthalene, methanol, and concentrated

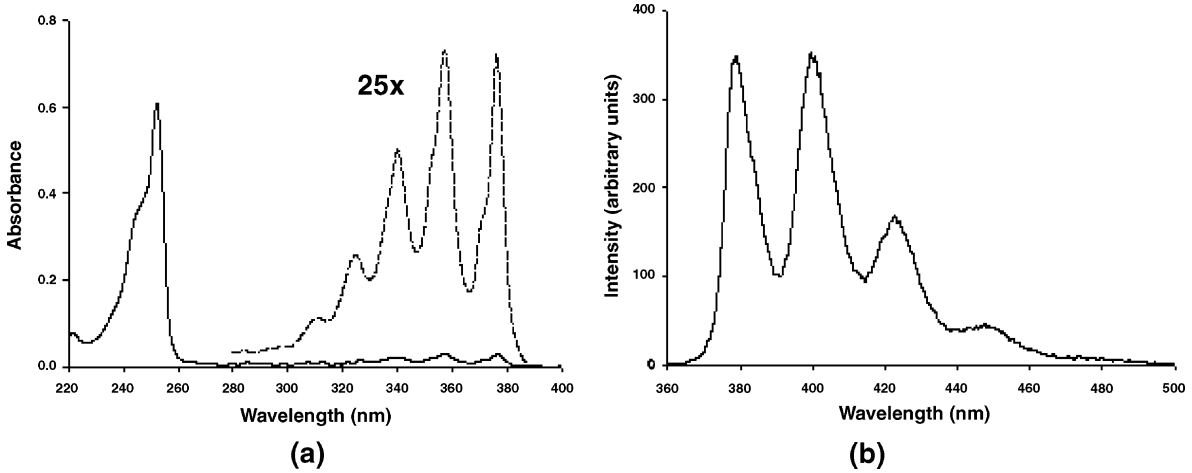

Figure 2. Absorbance (a) and emission (b) spectra of anthracene in methanol: (a) 3.4×10^{-4} and (b) 3.4×10^{-6} M concentration.

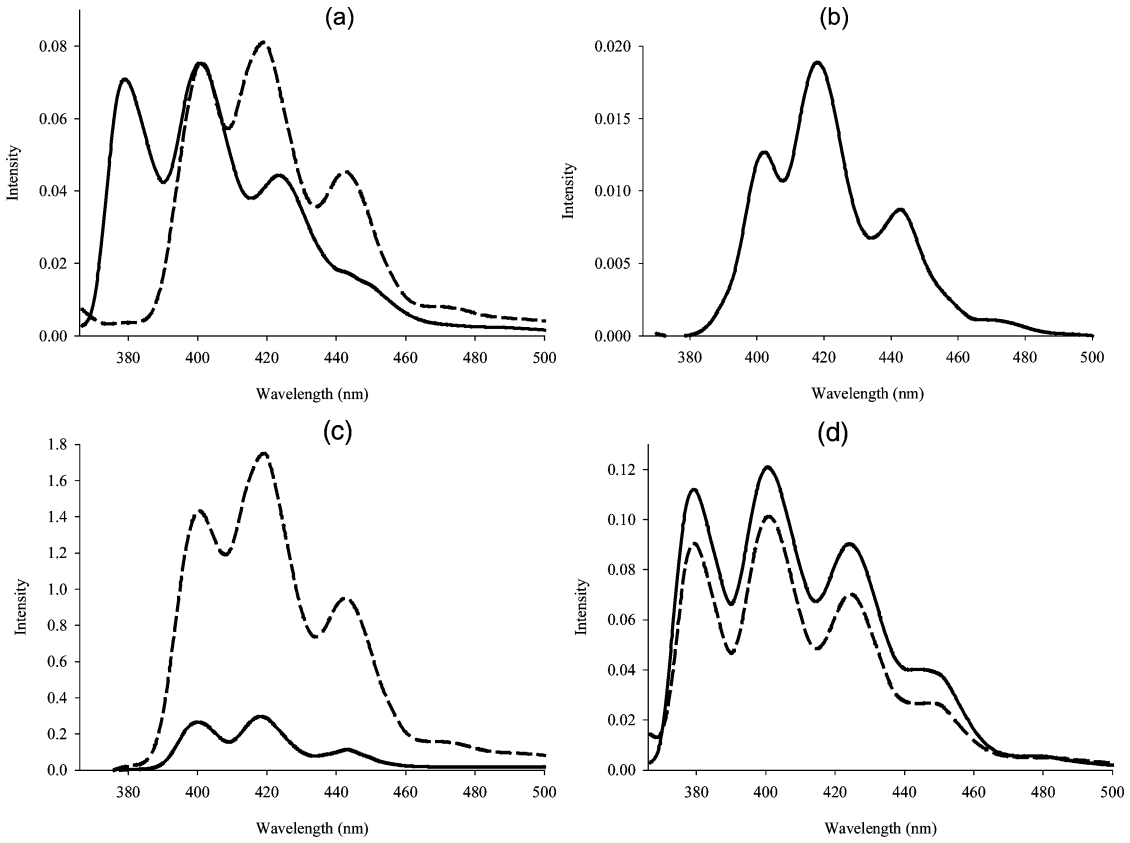

Figure 3. Anthracene fluorescence measured (a) at the water surface, after 30 min deposition (solid line) and 115 min deposition (dashed line) from the gas phase, (b) on a ground glass surface following evaporation of methanol solvent, (c) on ice, after 10 min deposition (solid line) and 45 min deposition (dashed line) from the gas phase, and (d) at the surface of liquid decanol at 24 °C (solid line) and on solid decanol at −8 °C (dashed line).

nitric acid were purchased from Caledon and had stated purities of 98%, 99.8%, and ≥99.9%, respectively. Laboratory grade 6% hydrogen peroxide was purchased from ACP. Ice was prepared from 18 mΩ deionized water. Nitrogen gas and oxygen gas were purchased from BOC and had stated purities >99.99%.

Results

Spectra. Figure 2 shows anthracene absorption and fluorescence spectra in dilute methanol solution. Its fluorescence spectrum in water is the same and remains unchanged as the solution concentration is increased up to 1.7×10^{-7} M (saturated solution in water) both within solution and at the water surface. In methanol, when the anthracene concentration exceeds ~7×10^{-6} M, the fluorescence peak at ~380 nm begins to decrease in intensity; this feature disappears almost completely once concentrations approach 10^{-3} M. Figure 3 shows anthracene fluorescence spectra at the surface of various substrates. When anthracene is deposited onto the water surface from the gas phase, the spectrum initially resembles that in water solution, but after 115 min of deposition the ~380 nm peak is no longer observed. This peak is not seen at all on ice, independent of the manner in which anthracene is introduced to the surface (i.e., deposited from the gas phase or frozen from solution), and also independent of the gas-phase deposition time or solution concentration of anthracene prior to freezing. This spectrum is similar to that seen for anthracene on a glass surface, as shown

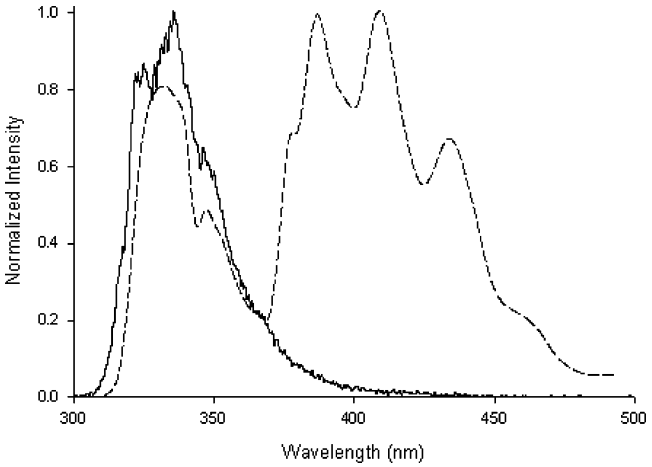

Figure 4. Intensity-normalized naphthalene fluorescence spectra measured in water solution (solid line) and on ice (dashed line).

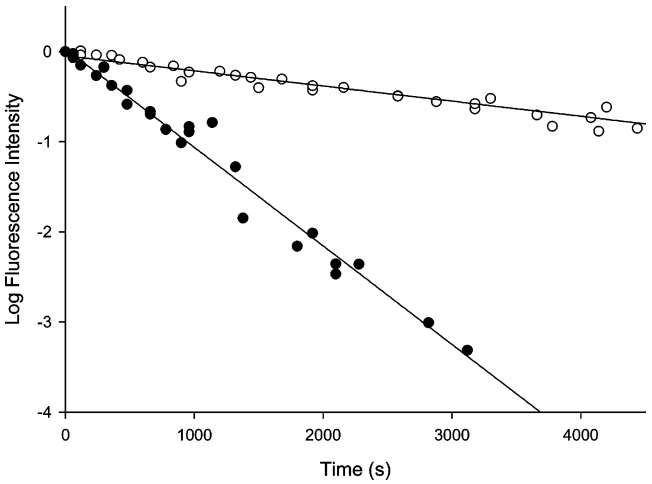

Figure 5. Plot of the time-dependent decay of fluorescence intensity from anthracene at the water surface (hollow circles) and at the ice surface (filled circles).

in Figure 3b. Conversely, at low deposition times ($\leq$7 min) on frozen decanol the 380 nm fluorescence peak has the same relative intensity as that observed at the liquid decanol surface, which in turn resembles that observed in and at the surface of dilute aqueous solutions. At high anthracene concentrations in solution and on all surfaces, a broad peak centered around 480 nm begins to appear.

Naphthalene fluorescence measured on the ice surface and in aqueous solution is shown in Figure 4. Intense emission at wavelengths higher than 400 nm is seen on ice but is not observed in water. The shapes of the fluorescence spectra of both anthracene and naphthalene remain unchanged after at least 80 min of irradiation on ice.

Direct Photolysis Kinetics. For the kinetic measurements, fluorescence intensity vs time data were fit to the function

$$I = I_0 e^{-k_{obs}t} + c \quad (1)$$

where c accounts for variations in the background signal level and k_{obs} yields the decay rate due to the reaction. When plotted logarithmically, this expression predicts that a linear dependence with time should be observed, if the reaction is first order with respect to PAH concentration. Figure 5 displays data obtained for anthracene photolysis at the surfaces of water and of ice. Whenever anthracene was introduced to the liquid or solid aqueous surface from the gas phase, exponential decays were observed at both 403 and 420 nm, and the data were well fit by using eq 1, as illustrated in Figure 5. When experiments were carried out with anthracene prepared in solution, either on water or on ice, first-order kinetic expressions fit the data very well, but in some cases second-order kinetic expressions also provided reasonable fits to the data.

TABLE 1: Observed Rate Constants for Anthracene Photolysis on Various Surfaces

substrate	attributes	k_{obs} (s^{-1}) [a]
water	deposited from gas (24 °C)	$(0.17 \pm 0.03) \times 10^{-3}$
	prepared in solution (24 °C)	$(0.17 \pm 0.04) \times 10^{-3}$
	prepared in solution (1 °C)	$(0.18 \pm 0.05) \times 10^{-3}$
ice	deposited from gas (−16 °C)	$(1.06 \pm 0.05) \times 10^{-3}$
	frozen from solution (−16 to −2 °C)	$(1.07 \pm 0.09) \times 10^{-3}$
glass	24 °C	$(0.13 \pm 0.04) \times 10^{-3}$
	−16 °C	$(0.4 \pm 0.1) \times 10^{-3}$
decanol	24 °C, liquid	$(0.26 \pm 0.05) \times 10^{-3}$
	−8 °C, solid	$(0.70 \pm 0.05) \times 10^{-3}$

[a] Errors represent one standard deviation.

TABLE 2: Observed Rate Constants for Naphthalene Photolysis in Water and on Ice

environment	k_{obs} (s^{-1})
water (bulk)	$(0.024 \pm 0.001) \times 10^{-3}$
ice (surface)	$(0.22 \pm 0.05) \times 10^{-3}$

TABLE 3: Observed Rate Constants of Anthracene Photolysis in the Presence of Various Cutoff Filters on Ice

filter cutoff	k_{obs} (s^{-1})
no filter	$(1.3 \pm 0.1) \times 10^{-3}$
295 nm	$(1.06 \pm 0.07) \times 10^{-3}$
320 nm	$(1.3 \pm 0.3) \times 10^{-3}$
360 nm	$<4 \times 10^{-5}$ [a]

[a] Established as an upper limit

Table 1 details the observed first-order rate constants for anthracene photolysis on each substrate. The photolysis rate on ice is over six times greater than that observed at the liquid water surface. The observed rate of reaction on liquid decanol is slightly greater than that on liquid water, and freezing the decanol gives rise to a factor-of-three photolysis rate enhancement. The rates of reaction observed on ice and on water are insensitive to the method of sample preparation, the wavelength at which fluorescence is monitored during the reaction, and the surface concentration of anthracene. Anthracene's photolysis rate on glass at room temperature is similar to that on liquid water. At −16 °C, however, the rate measured on glass surfaces increases by close to a factor of 3. At this temperature a thin layer of frost was observed on the glass surface, even when dry nitrogen was flowed across the sample.

First-order photolysis rate constants obtained for naphthalene are documented in Table 2. The rate on the ice surface is approximately nine times greater than that in water solutions.

Temperature and Wavelength Dependence. Photolysis kinetics were measured on ice at temperatures ranging from −16 to −2 °C, and on water at 1 and 24 °C. The observed rate constants on ice were identical within experimental uncertainty at each temperature. Likewise, no temperature dependence was observed for the kinetics at the water surface, as shown in Table 1.

The wavelength dependence for the photolysis kinetics of anthracene on ice was measured by substituting various optical filters for the 295 nm filter normally used. The results are displayed in Table 3. The decay rate observed with the 295 nm cutoff filter is the same as that seen with a 320 nm filter, or

TABLE 4: Effect of Nitric Acid and Hydrogen Peroxide on Anthracene Photolysis Rate Constants

substrate	additional compd	concentration	k_{obs} (s^{-1})
water	none	n/a	$(0.17 \pm 0.04) \times 10^{-3}$
surface	HNO_3	5×10^{-3} M	$(1.8 \pm 0.1) \times 10^{-3}$
	H_2O_2	7.2×10^{-3} M (24 °C)	$(0.73 \pm 0.06) \times 10^{-3}$
		7.2×10^{-3} M (1 °C)	$(0.90 \pm 0.05) \times 10^{-3}$
ice	none	n/a	$(1.06 \pm 0.07) \times 10^{-3}$
surface	HNO_3	$\leq 6.4 \times 10^{17}$ molecules (from gas)[a]	$(1.1 \pm 0.4) \times 10^{-3}$
		3.16 M	$(1.24 \pm 0.4) \times 10^{-3}$
		15.8 M	$(5.15 \pm 0.07) \times 10^{-3}$
	H_2O_2	7.2×10^{-3} M	$(1.03 \pm 0.08) \times 10^{-3}$

[a] Upper limit based on nitric acid room temperature vapor pressure and volume dispensed onto the ice.

TABLE 5: Effect of Oxygen on Observed Anthracene Photolysis Rate Constants on Ice

atmosphere	k_{obs} (s^{-1})
nitrogen	$(1.4 \pm 0.3) \times 10^{-3}$
air	$(1.06 \pm 0.07) \times 10^{-3}$
oxygen	$(3.1 \pm 0.1) \times 10^{-3}$

even that seen in the absence of any optical filter. Using a 360 nm cutoff filter reduces the rate of reaction to a value that we cannot measure. We estimate an upper limit for the rate constant under these illumination conditions of $\sim 4 \times 10^{-5}$ s^{-1}, based on the slowest rate we have been able to quantify. The observed wavelength dependence correlates reasonably well with anthracene's absorption spectrum in solution, shown in Figure 2a.

Indirect Photolysis. Table 4 compares the dependence of anthracene's photolysis rate on the presence of nitric acid and hydrogen peroxide on water and on ice. On the water surface, the presence of 5×10^{-3} M nitric acid increases the rate by an order of magnitude, and unpublished results from this lab show the same increase in photolysis rates in aqueous solutions of nitric acid. On ice, no change in the kinetics is seen when solutions of nitric acid of concentrations up to 3 M are deposited on the sample surface and frozen. A rate enhancement of a factor of 5 is observed when concentrated nitric acid (15.8 M) is frozen on the ice prior to introducing the anthracene solution. Introducing nitric acid from the gas phase does not increase the observed rate of reaction.

The photolysis rate of anthracene was measured on water and on ice in the presence of 7.2×10^{-3} M H_2O_2, which was either dissolved in the liquid solution or spread across the ice surface prior to introducing anthracene to the sample. The presence of H_2O_2 increases the observed rate of reaction by a factor of 4 on the water surface, but does not affect the rate on ice. No significant difference in the photolysis rate on the water surface was observed in the presence of H_2O_2 when the experiment was performed at 1 °C, versus when it was carried out at room temperature.

Effect of Oxygen. The effect of oxygen on anthracene photolysis kinetics on ice is displayed in Table 5. Purging the reaction chamber with oxygen prior to and during photolysis resulted in a factor of 3 increase in the observed photolysis rate over that measured in air, whereas purging the chamber in the same way with nitrogen resulted in only a very slight increase in the observed rate.

Discussion

Anthracene Surface Coverage. We may estimate the anthracene concentration on ice surfaces for the experiments involving gas-phase deposition as follows: We assume that anthracene's concentration in nitrogen is given by its room temperature equilibrium value (2×10^{13} molecules cm^{-3} based on its room temperature vapor pressure)[33] when it enters the reaction chamber, and that a steady-state concentration of gas-phase anthracene is maintained in the reaction chamber during deposition. If this is in equilibrium with the surfaces in the chamber, using an estimated snow−air partitioning coefficient K_{SA} for anthracene of $10^{-1.03}$ m,[34] based on a linear free energy relationship,[35] we then may estimate an anthracene concentration on our ice surface of 3×10^{11} molecules cm^{-2}. This value is well below the calculated saturated surface coverage of anthracene at the air−water interface of $\sim 1 \times 10^{13}$ molecules cm^{-2}.[36]

In our experiments, anthracene fluorescence intensity increased with increasing deposition time from the gas phase up to at least 75 min of deposition. This indicates that equilibrium partitioning between the gas phase and the ice surface had not been fully obtained in this time. Therefore, the anthracene surface coverage estimated based on equilibrium partitioning is likely an upper limit, since we rarely used deposition times greater than 30 min.

Spectra. In water, naphthalene fluoresces between ~310 and 380 nm, with maximum intensity at ~340 nm, as shown in Figure 4. This emission is also observed on the ice surface, but the major feature there is a new fluorescence band appearing to the red of 370 nm, which shows peaks at 387, 410, and 433 nm. This spectrum resembles the emission from excimeric naphthalene[37] observed at 77 K, and indicates that naphthalene self-associates readily on ice.

Fluorescence of monomeric anthracene at low temperatures (<77 K) displays two major peaks at 381 and 403 nm,[38] where the 381 nm peak corresponds to the 0−0 emission band.[38,39] We observe a similar spectrum in dilute solutions, with broader peaks and with additional peaks appearing at 420 and 450 nm. The same spectrum is seen at the air−water interface at low deposition times (<~30 min) in previous work,[36,40] and in this work as well, as shown in Figure 3a.

In more concentrated solutions, as well as on the water surface after long deposition times, the absolute intensity of the 380 nm peak begins to decrease, while the intensities of the other peaks continue to increase. This spectral shift can likely be attributed to self-association of anthracene: Crystalline anthracene does not fluoresce at 381 nm, and the greatest intensity shifts to the band at 420 nm,[39,41−43] as we see at high surface coverages on glass surfaces, and as others have observed on alumina and silica gel surfaces.[44,45] On ice, the fluorescence spectrum that we see even at the shortest deposition times resembles that of crystalline anthracene.

Anthracene is ~50% more polarizable than naphthalene,[46] and so is more likely to undergo self-association. This is supported by our observation of exclusively monomeric naphthalene emission in aqueous solution at concentrations where anthracene emission shows significant self-absorption of the 380 nm peak. Since naphthalene clearly undergoes self-association at the ice surface, anthracene's fluorescence spectrum at the ice surface most likely arises from the self-associated species as well.

A hallmark of anthracene self-association is a broadening and red shift of the absorption spectrum, as well as the appearance of a new absorption band at 390 nm.[44,45] Various features of anthracene's emission spectra on solid surfaces, including the appearance of bands at 420 nm[44] and 450 nm,[45] have also been ascribed to its self-association. However, we observe these bands in dilute aqueous and organic solutions at concentrations that

do not give rise to the changes in anthracene's absorption spectrum assigned to self-association. Further, the fluorescence intensities of these bands in solution show the same linear dependence on anthracene concentration as that displayed by the 403 nm band, which is a feature of monomer fluorescence.[38,39]

A reduction in fluorescence intensity of the ~380 nm band relative to longer wavelength bands[44,45] does appear to be due to self-association of anthracene. We observe a relative and an absolute reduction of the intensity of this band in concentrated solutions in methanol and octanol,[47] as well as after long loading times on a water surface, consistent with this phenomenon being due to reabsorption of light by self-associated anthracene, due to the red shift of its absorption spectrum.[44,45]

Emission at 380 nm has been observed on silica and alumina surfaces at surface coverages of up to 1%, while at higher coverages it is not observed.[44] On the basis of the calculation discussed above, we have estimated a maximum surface coverage of ~3% of a monolayer on ice. This concentration is evidently sufficient to suppress monomer emission. On glass, anthracene surface coverage exceeds that of a monolayer in our experiments, so we would not expect to see emission at 380 nm. The fact that emission from self-associated anthracene is observed at well below monolayer coverages on silica and alumina,[44,45] as well as after short periods of deposition from the gas phase on ice, could indicate that at submonolayer concentrations, anthracene is not distributed evenly across the substrate surface, but rather is present in "islands".

Anthracene's propensity to self-associate depends at least to some extent on the nature of the substrate. Although anthracene is quite insoluble in liquid water, it does not appear to self-associate appreciably on the water surface except at high concentrations. On ice and glass, anthracene seems to self-associate very readily, but on frozen decanol the fluorescence spectrum does not indicate more self-association than on liquid decanol. The observed self-association is clearly not strictly a temperature effect either, since the spectra on solid decanol were obtained at the same temperatures as several of those on ice.

The fact that we observe self-association of both anthracene and naphthalene on some solids after short gas-phase deposition times suggests that this could occur with other PAHs and on other solid surfaces as well. This could affect studies that monitor the kinetics of surface reactions, especially if there is a possibility that the self-associated species will display different kinetics than the monomeric species. This could also be important in polluted environments, where gas-phase deposition of PAHs frequently occurs.

Direct Photolysis Kinetics. Depositing PAHs from the gas phase ensures that they are present on the ice surface, presumably in the QLL, and not incorporated into the ice matrix. The fact that anthracene photolysis kinetics are identical for gas-deposited samples and those frozen from solution suggests that anthracene is also present in the QLL for experiments involving frozen PAH solutions. It should be noted that this does not exclude the possibility of reactions also occurring within the ice matrix under these conditions.

Unpublished data from this lab show identical photolysis rates for pyrene and anthracene in bulk aqueous solution as on the water surface, and it is quite possible that this behavior holds true for other PAHs as well. The enhanced anthracene and naphthalene photolysis rates on ice suggest that the environment presented to PAHs by the ice surface is different from that presented by liquid water. In the following sections of this paper we discuss some possible reasons for this difference.

Spectral Changes in Anthracene and Naphthalene. Like anthracene, crystalline naphthalene's absorbance spectrum is red-shifted with respect to the monomer.[48] Monomeric naphthalene absorbs only very weakly above 295 nm, but crystalline naphthalene absorbs much more strongly up to ~303 nm. This shift in absorbance is likely to enhance the naphthalene photolysis rate we observe, because in our system light at wavelengths below 295 nm is cut off by an optical filter. Therefore, the increase in naphthalene photolysis rate on ice compared to in water could be at least partially explained by a possible red shift in its absorbance spectrum on ice, where it is present primarily in a self-associated form.

Despite anthracene's self-association on ice, a red shift in its absorbance spectrum does not appear to enhance its photolysis rate: The observed photolysis rate on glass, where anthracene is also self-associated, is identical with that on water. The observed photolysis rate on frozen decanol is greater than that on liquid decanol, although the emission on both surfaces is that of monomeric anthracene. This suggests that factors other than increased reagent concentrations, which is thought to cause rate enhancements in frozen media for bimolecular reactions,[28] are responsible for our observed rate increases for anthracene on ice. Furthermore, first-order photolysis decay kinetics are observed in all instances, also suggestive that an increased anthracene concentration is not responsible for the observed rate increases.

The wavelength dependence of the kinetics for the reaction on ice is consistent with anthracene's absorption in solution, which suggests that anthracene's absorption intensity at wavelengths to the red of 360 nm is not greatly enhanced by the change in substrate. It is possible that the magnitude of absorption at wavelengths below 360 nm is enhanced on ice (i.e., anthracene's absorption cross section is greater) or that the photolysis quantum yield is increased for samples present at the ice surface. For example, Dubowski and Hoffmann[12] observed a 3-fold increase in the photolysis quantum yield of 4-nitrophenol in ice compared to that measured in water. Although no reason for this increase was proposed by those authors, such an increase could be more general. This possibility awaits further study.

Enhanced Photon Flux. The presence of reflected light at the ice surface could lead to an enhanced photon flux, which might explain the enhanced reaction rate on ice. In this case we would expect the enhancement to be molecule-independent if scattering is uniform with wavelength. However, naphthalene photolysis is nine times faster on ice than on water, and anthracene photolysis is six times faster on ice than on water. We would also expect to see an even faster rate on a surface that scatters light more efficiently than ice. Frozen decanol is such a surface, at least in the visible spectrum: Its surface appears white and rough, while the surface of the water ice appears clear and smooth. The amount of scattered light can be determined semiquantitatively by monitoring the intensity of stray 532 nm light arising from incomplete tripling of the Nd:YAG fundamental. The intensity at 532 nm observed in our experiment becomes more intense with increased scattering at the sample surface. The absolute intensity of this peak is much higher on ice than on water, and somewhat higher on frozen decanol than on ice. The rate of anthracene photolysis on frozen decanol, however, is only half that observed on ice. Although this does not exclude the possibility of an enhanced photon flux playing some role in the observed increase in rate on ice, it suggests that it is not the only factor.

Effect of Surface Polarity on Kinetics. PAH photodegradation rates have been observed to increase with increasing solvent polarity.[49,50] If there is a large presence of dangling OH bonds at the ice surface, this would increase its polarity compared to that of a liquid water surface,[51] and these dangling OH groups have in fact been observed spectroscopically.[26,52,53] However, these free OH groups are seen primarily in amorphous ice: When surface reconstruction occurs, as it does after annealing the surface to form crystalline ice, the number of dangling OH groups observed is significantly reduced.[52,53] Under these circumstances, the adsorption of N_2 to annealed ice surfaces becomes similar to adsorption to nonpolar surfaces such as Teflon,[54] suggesting that annealed ice, such as that used in our experiments, does not present an environment that is more polar than that of liquid water. We have recently used pyrene, a PAH with a polarity-dependent fluorescence spectrum, to compare the polarity of an ice surface with that of the water surface,[55] and the results indicate that the polarities of the two surfaces are in fact very similar. Using this same technique, we have previously observed large differences in polarity between the surfaces of liquid water and organic solvents,[36,56] even when the latter are only present at monolayer amounts at the water surface. These observations suggest that increased polarity is not responsible for our observed rate enhancement at the ice surface vs at the liquid water surface, although it could explain the faster rate observed on ice compared to on frozen decanol. However, a higher surface polarity does not always result in faster photolysis: Anthracene photolysis is faster at the liquid decanol surface than at the liquid water surface, even though decanol is very much less polar a molecule than water.

pH Dependence. Although we did not set out to determine the existence of a pH dependence for anthracene photolysis on ice, our indirect photolysis experiments used varying concentrations of nitric acid, and therefore spanned a range in pH below and including pH 7. The photolysis rates of PAHs generally increase with decreasing pH,[57,58] although anthracene has been observed to react more quickly at a higher pH in water.[57]

The anthracene photolysis rate in liquid water is linearly dependent on nitrate concentration, and therefore is almost certainly due to indirect photolysis rather than to an effect of pH. Since indirect photolysis appears to be unimportant on ice, we would expect to see a pH effect if it existed. However, we did not observe any significant variation in the kinetics in the presence of different nitric acid concentrations up to 3.16 M.

Effect of Oxygen. Debate continues regarding the role of molecular oxygen in the photolysis of PAHs. While some researchers have found, based on kinetics studies,[57] that the presence of molecular oxygen is unimportant to the photochemical fate of PAHs in aqueous solutions, others have observed photolysis rates to depend on oxygen concentration.[59−61] Proposed mechanisms for PAH photolysis in aqueous solutions invoke either direct ionization as the initial reaction step (Scheme 1),[60] or interaction with oxygen through electron transfer (Scheme 2), or the direct reaction of the excited triplet state formed by energy transfer to molecular oxygen (Scheme 3).[59,62,63]

Recently, Fasnacht and Blough[59] determined that anthracene and other PAHs in aqueous solutions do not undergo direct ionization under actinic radiation, so this mechanism can likely be discounted. Both of the other proposed photolysis mechanisms involve molecular oxygen, so it is likely that molecular oxygen is generally important to PAH photodegradation. However, its exact mechanistic role in these reactions, especially in the case of anthracene, remains unclear.

SCHEME 1

$$\mathrm{PAH} \xrightarrow[-e^-]{h\upsilon} \mathrm{PAH}^{\cdot+} \xrightarrow[-H^+]{H_2O} \text{Products}$$

SCHEME 2

$$\mathrm{PAH} \xrightarrow{h\upsilon} {}^1[\mathrm{PAH}]^* \xrightarrow[-e^-]{{}^3O_2} \mathrm{PAH}^{\cdot+} + O_2^- \xrightarrow[-H^+]{H_2O} \text{Products}$$

SCHEME 3

$$\mathrm{PAH} \xrightarrow{h\upsilon} {}^1[\mathrm{PAH}]^* \xrightarrow[\text{or } {}^1O_2^*]{{}^3O_2} {}^3[\mathrm{PAH}]^* + {}^1O_2^* \xrightarrow{{}^3O_2} \text{Products}$$

Anthracene photolysis kinetics in water exhibit odd behavior compared to other PAHs, in that the reaction rate increases both when oxygen concentrations are increased and when they are decreased.[57,59] This is as yet unexplained, and in fact there is not good agreement on the magnitude of the change in reaction rate brought on by varying the ambient oxygen concentration. Going from an air atmosphere to an oxygen atmosphere, rate increases of 20%,[57] 70%,[60] and ∼150%[59] have been reported. In experiments where kinetics were measured after purging the system with nitrogen, the rate enhancement was comparable to that obtained by purging the system with oxygen.[57,59] Inconsistent results under varying oxygen concentrations have been reported,[57] and we have observed this on the water surface as well: We consistently observe a photolysis rate increase in an atmosphere of oxygen, but the rates range from 30% to 110% faster than the rate observed in air.

On ice, we observe a small but reproducible increase in the rate relative to that in air (ca. 20%) when the reaction chamber is purged with nitrogen during freezing and throughout the reaction. Under an oxygen atmosphere we observe a reproducible increase in the reaction rate of a factor of 3. It is interesting that on ice we see a much smaller relative rate enhancement under nitrogen than under oxygen, compared to observations in water,[57,59] and also that the enhancement due to purging with oxygen is much larger than any seen in water.[57,59,60]

The enhancement of the rate under both an oxygen and a nitrogen atmosphere suggests that oxygen's role in anthracene photolysis is somewhat complex. Fasnacht and Blough[59] recently proposed that at high oxygen concentrations, PAH radical cations are formed via electron transfer to oxygen due to diffusional quenching of excited singlet state molecules, whereas at low oxygen concentrations the photodegradation occurs primarily by ground state molecular oxygen adding directly to excited triplet-state anthracene. They later suggested[64] that PAHs such as pyrene which have long-lived singlet states react primarily through the excited singlet state, whereas compounds with shorter singlet state lifetimes, such as anthracene, react primarily through the triplet state pathway. It is possible that on ice the importance of the singlet-state mechanism is increased for anthracene. This could explain at least some of the difference between the rates observed on ice and on water, since the more energetic singlet state has been seen to be more reactive than the triplet state.[64] In support of this idea, we have not observed quenching of anthracene fluorescence by the ice surface compared to the water surface, whereas we have observed this for other small PAHs, such as pyrene and acridine.[55]

If the ice surface increases the relative importance of the excited singlet state reaction, it is not due to anthracene's self-association on the surface or to the fact that the ice surface is solid. This is evidenced by the slow reaction observed on a glass surface, where anthracene shows efficient self-association. The rate enhancement on frozen decanol shows that this effect is not unique to water ice, and that rate enhancement can occur

when anthracene emission indicates that anthracene is present in the monomeric form.

Although the reason for the faster photolysis rates on ice and frozen decanol compared to on glass is not known, it is possible that dissolved molecular oxygen plays a role. If dissolved oxygen interacts more efficiently with PAHs than does gas-phase oxygen, we would expect the reaction on glass to be slower than reactions on ice and frozen decanol, which may contain oxygen in their QLLs. One of our observations supports this idea: On ice, the 20% rate enhancement under a nitrogen atmosphere compared to under air is only observed when the chamber is purged with nitrogen during freezing. No change is observed if nitrogen is introduced to the chamber once the ice is already formed. It is possible that the oxygen content in the ice (or the QLL) influences photolysis kinetics more than that in the overlying atmosphere. This observation could also explain oxygen's greater effect on ice than in water: Equilibrium partitioning calculations indicate that oxygen partitions more than twice as effectively into water at −15 °C than water at 25 °C.

Indirect Photolysis Kinetics. Reaction with hydroxyl is the primary means of chemical transformation of PAHs in the atmosphere,[33] and OH radicals are very important oxidizers in natural waters.[65] On ice, as well as in aqueous solutions, OH radicals are formed from the photolysis of nitrate and of hydrogen peroxide.[5] The presence of hydrogen peroxide has been shown to be much less important to the photolysis rate of monochlorophenols in ice than in aqueous solutions,[30] and here we have extended this observation to anthracene. We also observe an insensitivity of the kinetics to the presence of nitric acid on ice.

It has been suggested that the insensitivity of the kinetics to the presence of H_2O_2 on ice could be due to changes in its optical absorption properties on ice,[30] but other researchers[5,18] have measured temperature dependences of the photolysis quantum yields for H_2O_2 and NO_3^- in water and in ice that argue against this: On the basis of their measured temperature dependences, going from 24 to −16 °C, one would expect a 4-fold reduction in the amount of hydroxyl produced from NO_3^- photolysis, and a 40% reduction in the amount of hydroxyl produced from H_2O_2 photolysis. In our study, the presence of 5×10^{-3} M HNO_3 caused a 10-fold increase in the observed anthracene photolysis rate constant on water, but HNO_3 concentrations 3 orders of magnitude higher did not affect the kinetics on ice. Likewise, 7.2×10^{-3} M H_2O_2 caused an increase of a factor of 4 in the observed rate constant on the liquid water surface; even accounting for the 40% reduction in the quantum yield of OH radicals expected based on Chu and Anastasio's proposed temperature dependence,[18] an enhancement of at least a factor of 2 should be observed with this concentration of H_2O_2 on ice.

The insensitivity to temperature of the kinetics for the reaction on H_2O_2 solutions suggests that the different behavior observed on ice is due to physical characteristics of the ice surface rather than to a temperature effect. We present several possible explanations for the lack of indirect photolysis observed on ice. The first is that the diffusion of both anthracene and hydroxyl is likely much lower on ice than on liquid water, leading to fewer collisions and therefore reactions. This has also been suggested by Klanova et al.[30] As well as a reduction in the diffusion coefficients, one would expect a smaller reaction rate. However, the insensitivity to temperature in water argues against that.

The second possibility is that very little H_2O_2 remains on the ice: H_2O_2 partitioning to ice surfaces is very inefficient.[51] This cannot, however, be extended to explain the insensitivity of the kinetics to nitric acid: This compound adsorbs strongly to ice surfaces,[66,67] and we have observed its presence at ice surfaces when it is both frozen from solution and deposited from the gas phase.[55]

It is also possible that once OH radicals are produced, they could become bound to the ice surface, and be rendered unavailable for reaction with anthracene. The presence of hydroxyl has not been directly measured in ice after photolysis of nitrate or hydrogen peroxide. Chu and Anastasio[5,18] detected OH radicals by using benzoic acid as a chemical probe and measuring the reaction products of benzoic acid and hydroxyl after melting irradiated ice samples. If OH radicals are bound to the ice surface, during melting they could be released and become accessible for reaction. This could explain why Chu and Anastasio see evidence of hydroxyl reacting with benzoic acid, while we do not see any evidence of hydroxyl reacting with anthracene on ice.

The recombination of OH radicals to form H_2O_2 is thought to be a major mechanism of H_2O_2 formation in interstellar ice;[68,69] this process could significantly reduce the effect of H_2O_2 on the photolysis rate of PAHs. The recombination of OH radicals on ice likely occurs at close to a diffusion-limited rate.[69] Hydroxyl radicals could also recombine with NO_2 radicals to reform nitric acid when that compound is the hydroxyl source. In Chu and Anastasio's experiments,[5,18] the benzoic acid concentrations always exceeded the nitrate/hydrogen peroxide concentrations to ensure that every OH radical would react with a benzoic acid molecule. An excess of benzoic acid would also reduce the likelihood of OH radicals recombining to form H_2O_2 by increasing the chances of them encountering, and then reacting with, a benzoic acid molecule. In our experiments, where anthracene concentrations were always orders of magnitude lower than nitric acid or hydrogen peroxide concentrations, OH radicals could be more likely to encounter one another than to encounter an anthracene molecule, and thus recombination could be their most important fate.

In many of our experiments involving nitric acid, deposited from the gas phase or frozen from solution, we likely had greater than monolayer coverage (2×10^{14} molecules cm^{-2}).[66] Phase diagrams for nitric acid and water ice[31,66] suggest that under these conditions, a liquid HNO_3/H_2O solution will exist at the ice surface. Although in aqueous nitric acid solutions the nitric acid concentrations used give rise to significant photolysis rate increases, we do not observe any change in the kinetics on ice. This indicates that despite the possible presence of a liquid solution at the ice surface, the environment seen by anthracene remains similar to that on pure water ice.

Conclusions

Anthracene and naphthalene show significant enhancements in photolysis rates on ice surfaces compared to those observed on or in water. These enhancements are insensitive to the means of introducing the PAH to the ice surface, to the method of ice preparation, and to temperature. Although both anthracene and naphthalene self-associate very readily on frozen water surfaces, this self-association does not appear to affect the reaction kinetics. These results are consistent with an increased absorption cross section and/or photolysis quantum yield on ice compared to water surfaces.

The presence of molecular oxygen has a larger effect on anthracene's photolysis rate on ice than on or in water. In a

pure oxygen atmosphere, a 3-fold increase in the photolysis rate is observed compared to the rate in air, which is much larger than any enhancement observed in liquid water under oxygen. A smaller increase in the photolysis rate, of ca. 20%, is observed in a pure nitrogen atmosphere.

Indirect photolysis initiated by nitric acid and hydrogen peroxide are unimportant to anthracene photolysis kinetics on ice, although it is known that hydroxyl is formed from the photolysis of both these compounds in ice. Thus, although hydroxyl does not appear to react at an appreciable rate with anthracene in ice, it is possible that when the ice melts, the previously formed OH radicals will be available for reaction, and their effect on PAH photolysis rates in liquid water may then be significant.

Polycyclic aromatic hydrocarbons such as anthracene and naphthalene are present in relatively low concentrations in high latitude snowpacks, and their chemical fate in frozen media has not been examined. Their concentrations in urban snows, however, are much higher,[33,70] as are the concentrations of other pollutants, including nitric acid, which could affect their chemical fate. Because the reaction products of PAHs are often more toxic than their parent compounds,[14,15] the introduction of these products into groundwater through snowmelts[71] is an important health concern. Despite their importance, the fate of organic pollutants in urban snow and ice has not yet been explored.

Acknowledgment. This work was funded by CFCAS and NSERC. The authors wish to thank Dr. T. Bartels-Rausch for his assistance with experimental design, and E. Morris for his contributions to data handling.

References and Notes

(1) Bernstein, M. P.; Dworkin, J. P.; Sandford, S. A.; Allamandola, L. J. Ultraviolet irradiation of the polycyclic aromatic hydrocarbon (PAH) naphthalene in H_2O. Implications for meteorites and biogenesis. In *Space Life Sciences*: *Extraterrestrial Organic Chemistry*, *UV Radiation on Biological Evolution, and Planetary Protection*; Elsevier: New York, 2002; Vol. 30, pp 1501.

(2) Elsila, J. E.; Hammond, M. R.; Bernstein, M. P.; Sandford, S. A.; Zare, R. N. *Meteorit. Planet. Sci.* **2006**, *41*, 785.

(3) Domine, F.; Shepson, P. B. *Science* **2002**, *297*, 1506.

(4) Bottenheim, J. W.; Fuentes, J. D.; Tarasick, D. W.; Anlauf, K. G. *Atmos. Environ.* **2002**, *36*, 2535.

(5) Chu, L.; Anastasio, C. *J. Phys. Chem.* **2003**, *107*, 9594.

(6) Dibb, J. E.; Huey, L. G.; Slusher, D. L.; Tanner, D. J. *Atmos. Environ.* **2004**, *38*, 5399.

(7) Dubowski, Y.; Colussi, A. J.; Hoffmann, M. R. *J. Phys. Chem. A* **2001**, *105*, 4928.

(8) Foster, K. L.; Plastridge, R. A.; Bottenheim, J. W.; Shepson, P. B.; Finlayson-Pitts, B. J.; Spicer, C. W. *Science* **2001**, *291*, 471.

(9) Boudries, H.; Bottenheim, J. W.; Guimbaud, C.; Grannas, A. M.; Shepson, P. B.; Houdier, S.; Perrier, S.; Domine, F. *Atmos. Environ.* **2002**, *36*, 2573.

(10) Dibb, J. E.; Arsenault, M. *Atmos. Environ.* **2002**, *36*, 2513.

(11) Sumner, A. L.; Shepson, P. B.; Grannas, A. M.; Bottenheim, J. W.; Anlauf, K. G.; Worthy, D.; Schroeder, W. H.; Steffen, A.; Domine, F.; Perrier, S.; Houdier, S. *Atmos. Environ.* **2002**, *36*, 2553.

(12) Dubowski, Y.; Hoffmann, M. R. *Geophys. Res. Lett.* **2000**, *27*, 3321.

(13) Klan, P.; Klanova, J.; Holoubek, I.; Cupr, P. *Geophys. Res. Lett.* **2003**, *30*, 46.

(14) Klanova, J.; Klan, P.; Nosek, J.; Holoubek, I. *Environ. Sci. Technol.* **2003**, *37*, 1568.

(15) Klan, P.; Holoubek, I. *Chemosphere* **2002**, *46*, 1201.

(16) Robinson, C.; Boxe, C. S.; Guzman, M. I.; Colussi, A. J.; Hoffmann, M. R. *J. Phys. Chem. B* **2006**, *110*, 7613.

(17) Heger, D.; Klanova, J.; Klan, P. *J. Phys. Chem. B* **2006**, *110*, 1277.

(18) Chu, L.; Anastasio, C. *J. Phys. Chem. A* **2005**, *109*, 6264.

(19) Beaglehole, D.; Nason, D. *Surf. Sci.* **1980**, *96*, 357.

(20) Doppenschmidt, A.; Butt, H.-J. *Langmuir* **2000**, *16*, 6709.

(21) Elbaum, M.; Lipson, S. G.; Dash, J. G. *J. Cryst. Growth* **1993**, *129*, 491.

(22) Engemann, S.; Reichert, H.; Dosch, H.; Bilgram, J.; Honkimaki, V.; Snigirev, A. *Phys. Rev. Lett.* **2004**, *92*, 205701.

(23) Golecki, I.; Jaccard, C. *Phys. Lett.* **1977**, *63A*, 374.

(24) Lied, A.; Dosch, H.; Bilgram, J. H. *Phys. Rev. Lett.* **1994**, *72*, 3554.

(25) Sadtchenko, V.; Ewing, G. E. *J. Chem. Phys.* **2002**, *116*, 4686.

(26) Wei, X.; Miranda, P. B.; Shen, Y. R. *Phys. Rev. Lett.* **2001**, *86*, 1554.

(27) Rosenberg, R. *Phys. Today* **2005**, *58*, 50.

(28) Pincock, R. E. *Acc. Chem. Res.* **1969**, *2*, 97.

(29) Literak, J.; Klan, P.; Heger, D.; Loupy, A. *J. Photochem. Photobiol. A* **2003**, *154*, 155.

(30) Klanova, J.; Klan, P.; Heger, D.; Holoubek, I. *Photochem. Photobiol. Sci.* **2003**, *2*, 1023.

(31) Hanson, D.; Mauersberger, K. *J. Phys. Chem.* **1988**, *92*, 6167.

(32) Handley, S.; Clifford, D.; Donaldson, D. J. *Atmos. Environ.* Submitted for publication.

(33) Finlayson-Pitts, B. J.; Pitts, J. N. *Chemistry of the Upper and Lower Atmosphere*; Academic Press: San Diego, CA, 2000.

(34) Lei, Y. D.; Wania, F. *Atmos. Environ.* **2004**, *38*, 3557.

(35) Roth, C. M.; Goss, K.-U.; Schwarzenbach, R. P. *Environ. Sci. Technol.* **2004**, *38*, 4078.

(36) Mmereki, B. T.; Chaudhuri, S. R.; Donaldson, D. J. *J. Phys. Chem. A* **2003**, *107*, 2264.

(37) Kawakubo, T.; Okada, M.; Shibata, T. *J. Phys. Soc. Jpn.* **1966**, *21*, 1469.

(38) Nakhimovsky, I.; Lamotte, M.; Joussot-Dubien, J. *Handbook of low temperature electronic spectra of polycyclic aromatic hydrocarbons*; Elsevier: New York, 1989.

(39) Macnab, M. R.; Sauer, K. *J. Chem. Phys.* **1970**, *53*, 2805.

(40) Mmereki, B. T.; Donaldson, D. J.; Gilman, J. B.; Eliason, T. L.; Vaida, V. *Atmos. Environ.* **2004**, *38*, 6091.

(41) Chandross, E. A.; Ferguson, J. *J. Chem. Phys.* **1966**, *45*, 3564.

(42) Horiguchi, R.; Iwasaki, N.; Maruyama, Y. *J. Phys. Chem.* **1987**, *91*, 5135.

(43) Mitani, T.; Yamanaka, T.; Suzui, M.; Horigome, T.; Hayakawa, K.; Yamazaki, I. *J. Lumin.* **1988**, *39*, 313.

(44) Dabestani, R.; Ellis, K. J.; Sigman, M. E. *J. Photochem. Photobiol. A* **1995**, *86*, 231.

(45) Wilkinson, F.; Worrall, D. R.; Williams, S. L. *J. Phys. Chem.* **1995**, *99*, 6689.

(46) Staikova, M.; Messih, P.; Lei, Y. D.; Wania, F.; Donaldson, D. J. *J. Chem. Eng. Data* **2004**, *50*, 438.

(47) Kahan, T. F.; Kwamena, N.-O. A.; Donaldson, D. J. *Atmos. Environ.* **2006**, *40*, 3448.

(48) Bree, A.; Thirunamachandran, T. *Mol. Phys.* **1962**, *5*, 397.

(49) Low, G. K.-C.; Batley, G. E.; Brockbank, C. I. *J. Chromatogr.* **1986**, *392*, 199.

(50) Schmidt, R. *J. Phys. Chem. A* **2006**, *110*, 5990.

(51) Abbatt, J. P. D. *Chem. Rev.* **2003**, *103*, 4783.

(52) Roberts, J. T. *Acc. Chem. Res.* **1998**, *31*, 415.

(53) Schaff, J. E.; Roberts, J. T. *J. Phys. Chem.* **1996**, *100*, 14151.

(54) Adamson, A. W.; Dormant, L. M.; Orem, M. *J. Colloid Interface Sci.* **1967**, *25*, 206.

(55) Kahan, T. F.; Reid, J. P.; Bartels-Rausch, T.; Donaldson, D. J. To be submitted for publication.

(56) Mmereki, B. T.; Donaldson, D. J. *Phys. Chem. Chem. Phys.* **2002**, *4*, 4186.

(57) Lehto, K.-M.; Vuorimaa, E.; Lemmetyinene, H. *J. Photochem. Photobiol. A* **2000**, *136*, 53.

(58) Miller, J. S.; Olejnik, D. *Water Res.* **2001**, *35*, 233.

(59) Fasnacht, M. P.; Blough, N. V. *Environ. Sci. Technol.* **2003**, *37*, 5767.

(60) Sigman, M. E.; Zingg, S. P.; Pagni, R. M.; Burns, J. H. *Tetrahedron Lett.* **1991**, *32*, 5737.

(61) Mill, T.; Mabey, W. R.; Lan, B. Y.; Baraze, A. *Chemosphere* **1981**, *10*, 1281.

(62) Barbas, J. T.; Sigman, M. E.; Dabestani, R. *Environ. Sci. Technol.* **1996**, *30*, 1776.

(63) Mallakin, A.; Dixon, D. G.; Greenberg, B. M. *Chemosphere* **2000**, *40*, 1435.

(64) Fasnacht, M. P.; Blough, N. V. *Aquat. Sci.* **2003**, *65*, 352.

(65) Lam, M. W.; Tantuco, K.; Mabury, S. A. *Environ. Sci. Technol.* **2003**, *37*, 899.

(66) Abbatt, J. P. D. *Geophys. Res. Lett.* **1997**, *24*, 1479.

(67) Diehl, K.; Mitra, S. K.; Pruppacher, H. R. *Atmos. Environ.* **1995**, *29*, 975.

(68) Pan, X.; Bass, A. D.; Jay-Gerin, J.-P.; Sanche, L. *Icarus* **2004**, *172*, 521.

(69) Zheng, W.; Jewitt, D.; Kaiser, R. I. *Astrophys. J.* **2006**, *639*, 534.

(70) Becker, S.; Halsall, C. J.; Tych, W.; Hung, H.; Attewell, S.; Blanchard, P.; Li, H.; Fellin, P.; Stern, G.; Billeck, B.; Friesen, S. *Environ. Sci. Technol.* **2006**, *40*, 3217.

(71) Herbert, B. M. J.; Villa, S.; Halsall, C. J. *Ecotoxicol. Environ. Saf.* **2006**, *63*, 3.